

Multiphase flow performance in the wellbore

Mahmoud Elsharafi¹, Abigail Reyes¹, Till Gebel¹, Tapiwa Gassler¹, Abdulhadi Alsadi¹, Jibriel Abusaleem²

Email: jabusaleem@su.edu.ly

¹McCoy School of Engineering, Midwestern State University, Wichita Falls, TX 76308, USA¹

²Sirte University, Sirte, Libya

Abstract

Multiphase flow is found in various places both in nature and in practice, but multiphase flow is especially seen in the oil field operation. It occurs in oil and gas wells, gathering systems and many piping systems. The presence of liquid (oil/water) and gas must be accounted for when designing and predicting flow patterns in both wells and pipelines. Gas-liquid two phase flows are generally difficult to examine, model and predict in that the interactions between the phases are fairly complex and at times chaotic. In this paper, the behavior of multiphase flow in a piping system is investigated through both experimental and simulated methods. For experiments an undulating piping system was built to study vertical, horizontal and inclined sections. Experimental studies consist of studying and examining flow regimes in a complex piping system that models wellbore flow behavior. Furthermore, theoretical studies consist of complex two-phase flow simulations of pressure loss throughout the system. These experimental and theoretical studies help further understand the complexities of multiphase phenomenon.

Keywords: *Multiphase flow, Experimental, simulated, methods, pressure, studding, examining.*

1. Introduction

Multiphase flow term refers to any fluid flow consisting of more than one phase or component. Multiphase flow is found in various places. Found in both nature and in practice multiphase flow is especially seen in the petroleum industry. It occurs in oil and gas wells, gathering systems and many piping systems. Multiphase flow has been studied for many years dating back to 1977 when Stuhmiller first studied the pressure difference for potential flows. Later in 1997, Zhang and Prosperetti found that phase interactions also result in stress in a potential flow. In multiphase flow, the volume in the pipe occupied by a phase is often different from its proportion of the total volumetric flow rate. For a typical two-phase upward flow of gas, g, and liquid, l, where the less dense gas phase, g, will flow faster than

the denser liquid phase, l , there is a result “slip” or “hold up” effect due to differences in flow velocity causing the in-situ volume fraction of each phase to differ from the input volume fraction of the pipe. The denser phase is “held up” in the pipe relative to the lighter phase (Akintola 2014). The problem of accurately predicting pressure drops in flowing or gas-lift wells has given rise to many specialized solutions for limited conditions, but not to any generally accepted one for broad conditions. The reason for these many solutions is that the two-phase flow is complex and difficult to analyze even for the limited conditions studied.

Under some conditions, the gas moves at a much higher velocity than the liquid. As a result, the down-hole flowing density of the gas-liquid mixture is greater than the corresponding density, corrected for down-hole temperature and pressure, that would be calculated from the produced gas-liquid ratio. Also, the liquid's velocity along the pipe wall can vary appreciably over a short distance and result in a variable friction loss. Under other conditions, the liquid is almost completely entrained in the gas and has very little effect on the wall friction loss. The difference in velocity and the geometry of the two phases strongly influence pressure drop. These factors provide the basis for categorizing two-phase flow. The generally accepted categories (flow regimes) of two-phase flow are bubble, slug, (slug-annular) transition and annular-mist. They are ideally depicted in Fig. 1 and briefly described as follows (Orkiszewski 1967). Multiphase flows play an important role in many natural processes and engineering applications. They occur in a variety of environmental phenomena like rain, fog, snow, avalanches, soil erosion, and landslides, among others. Very critical biological and medical flows like blood flow is a multiphase flow, virtually every processing technology deals with multiphase flows. The flow of multiphase mixtures is a common phenomenon in industrial plants, such as chemical reactors and power generation units. It is considered to be an important phenomenon in the oil and gas industry from the energy point of view (Okoye 2016).

Varies studies were conducted to characterizes significant parameters that can describe the multi-phase flow mixture. Different models have been used to predict the flow patterns. Although, there many studies imply different approaches to investigate the pressure drop. Choi et al (2003), obtained data of flow regimes, void fraction, and frictional pressure drop in normal gravity, microgravity and hyper-gravity (2g) aboard a MU-300 aircraft. They concluded that the gravity dependency on flow regimes was more clearly seen as a gas and liquid flow rates decrease. The effect of gravity on two phase flow was insignificant for the turbulent flow regions. Curtis and Coffield (1999) investigated two phase flow pressure drop of high quality steam. Two phase pressure drop across a straight test pipe was experimentally determined for Reynolds number (Re) steam flow of a flow quality of 0.995 to 1.0. The testing described was been performed in order to reduce uncertainties associated with the effects of two phase flow on pressure drop. The two phase pressure drop data obtained in this test enhanced development of a correlation between friction factor, Reynolds number and flow quality. Fore et al (1997) presented measurements on both fluid flow and heat transfer for two phase slug flows in microgravity; they used air and two liquids (water and 50% aqueous glycerine solution) to obtain a range of liquid Reynolds numbers from 1000 to 20,000 in a 25.4mm inner diameter tube. They showed based on a comparison of microgravity to normal gravity correlations that the heat transfer coefficients are smaller in reduced gravity than in normal gravity under the same flow conditions. They summarized that smaller liquid phase turbulence levels in the gas and liquid can explain this difference.

Hannah et al (2012), through their research in computational fluid dynamics analysis of two-phase fluid flow in a packed Bed reactor which included the use of CFD in simulating an experiment on multiphase flow to compare results on flow regime and pressure drop. Their results included discussion of the programs capabilities for conducting analysis and comparison of simulated flow parameters against experimentally determined values. James and Silberman (1958) conducted a study on two phase flow in horizontal pipes with special reference to bubbly mixtures. It was found that the friction factor of what is approximately equal or slightly greater than the friction factor for liquid flowing alone in the mean velocity of the liquid while their size is inversely proportional to the square root of the pipe diameter. Kamp et al (2009) developed a mechanistic model for bubble coalescence in turbulent flow. Their model can be used to predict pressure drop in pipes. Their data was validated by data obtained in a reduced gravity aircraft. They concluded that in the absence of gravity, collisions between bubbles are smaller than the length scale of turbulence are primarily due to turbulence. Manmatha et al (2012) used computational fluid dynamics (CFD) modelling to evaluate the pressure drop caused by two phase flow of oil/water emulsions through sudden contractions. They obtained that the loss coefficients for the emulsions are found to be independent of the concentrations and type of emulsions. The numerical results were validated against experimental data and were found to be in good agreement. Wang et al (2004) presented data on the interfacial friction factor and relative interfacial roughness on the gas-liquid interface of an air-water annular flow in a tube with inner diameter of 9.525mm². Their results show that while the roughness in microgravity is less than half of that in normal gravity, the friction factor was only about 10% smaller in microgravity than that in normal gravity. The goal of this study is to obtain the pressure loss in a straight pipe of two-phase flow using a homogenous model and show the influence of the pressure drop on the fluid flow. The flow station is operational in Nigeria 's Niger Delta region and readings were collected from flow measurements during the study.

Early prior research demonstrated the superiority of ceramics for bearings and the existence of elasto- hydrodynamic (ehd) lubricant films at ball and roller contacts, the calculation of which is now an accepted part of bearing engineering. These new concepts are now used in the design of lubrication systems with solid lubricants that operate in much more severe environments than oils and greases. Proprietary computer codes and unique patented bearing configurations for optimizing the performance of bearing/solid-lubricant systems have been developed. In this way, patented self-contained solid-lubricated all-steel and hybrid-ceramic ball and roller bearings are now available for environments that do not contribute to their lubrication, such as in air or vacuum.

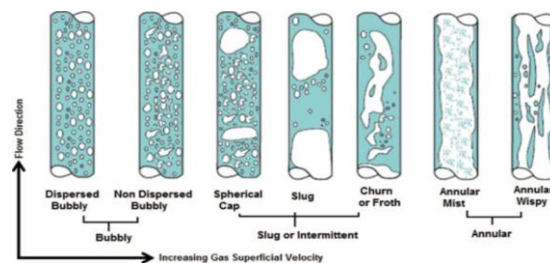


Figure 1: S. Farman Ali & H. Yeung (2015)

2- THEORY

Pressure Gradient

For this project one of the main concerns was the determination of pressure losses experienced throughout the system. In order to calculate these pressure losses, the Lockhart-Martinelli method was used. The following steps shown below are used to ultimately find the total multiphase Pressure Gradient.

In order to find the pressure gradient, the Cross- Sectional Area, A_c is determined

$$A_c = D_H^2$$

The Mass Flux, j can then be calculated

$$j = \frac{\dot{m}}{A_c}$$

Once Mass Flux is calculated the Reynolds number, Re_{H_2O} is determined

$$R_{H_2O} = \frac{j * D_H}{\mu}$$

Find friction factor, f_{H_2O} is also calculated from Reynolds number

$$f_{H_2O}^{-0.5} = -1.8 \log_{10} \left(\left(\frac{e}{3.7 D_H} \right)^{1.11} + \left(\frac{6.9}{R_{H_2O}} \right) \right)$$

Lastly the pressure gradient, $(\Delta P/L)_{H_2O}$ is calculated

$$\left(\frac{\Delta P}{L} \right)_{H_2O} = \frac{f_{H_2O} * (j_{H_2O})^2}{2 * \rho_{H_2O} * D_H}$$

Lockhart-Martinelli Parameter

From the Pressure Gradient $\left(\frac{\Delta P}{L} \right)$ the Lockhart-Martinelli parameter, X is given by:

$$X = \sqrt{\frac{\left(\frac{\Delta P}{L} \right)_{H_2O}}{\left(\frac{\Delta P}{L} \right)_{air}}}$$

Total Multiphase Pressure Gradient

First the Water Pressure Gradient Multiplier (Chisholm Equation), ϕ_{H_2O} is given by:

$$\phi_{H_2O} = (1 + 18X^{-1} + X^{-2})^{0.5}$$

Then, the Air Pressure Gradient Multiplier (Chisholm Equation) ϕ_{air} , is also given by:

$$\phi_{air} = (1 + 18X^{-1} + X^{-2})^{0.5}$$

Finally the Multiphase Pressure Gradient, $(\Delta P/L)_{multi}$ can be found by the following equation:

$$\left(\frac{\Delta P}{L} \right)_{multi} = \phi_{H_2O}^2 * \left(\frac{\Delta P}{L} \right)_{H_2O} = \phi_{air}^2 * \left(\frac{\Delta P}{L} \right)_{air}$$

Moody Chart

Once the Reynolds number and Friction factor are determined the appropriate flow that can be expected is determined from the moody diagram shown below.

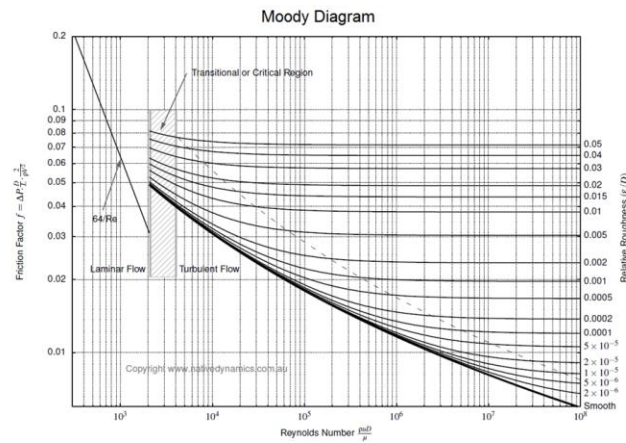


Figure 2: Kleinstreuer C. Modern Fluid Dynamics. Springer

From the moody diagram it can be determined that for our Reynolds Number, Friction Factor and Relative Roughness we will experience Turbulent Flow.

SIMULATION METHODS

Model Geometry

ANSYS was used to simulate both pressure losses and velocity magnitudes throughout the system. The Computational Fluid Dynamic (CFD) approach in fluent was used for both all of the simulations. For our mechanistic model we used a series of 2-foot-long pipes with an inner diameter of 1.5 inches as shown in the figure 3

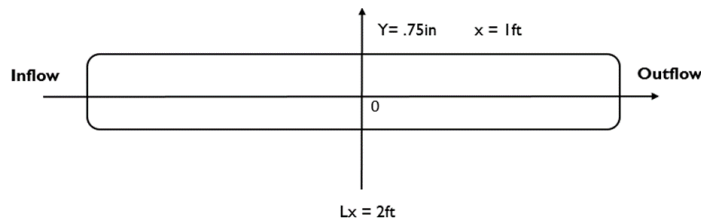


Figure 3: Mechanistic Model

Figure 4 illustrates a sample of the generated mesh. A max skewness value of .9 was used for the experiment.



Figure 4: Mesh

3- Experimental

Experimental methods consisted of the design and assembly of an undulating pipe system apparatus. As shown in figure 5 the open channel system consists of 2ft long, 1.5in diameter pipes installed in series emptying into a water tank. The apparatus was designed in a manner to include all three directions: horizontal, vertical and inclined. The two phases used were compressed air and water.

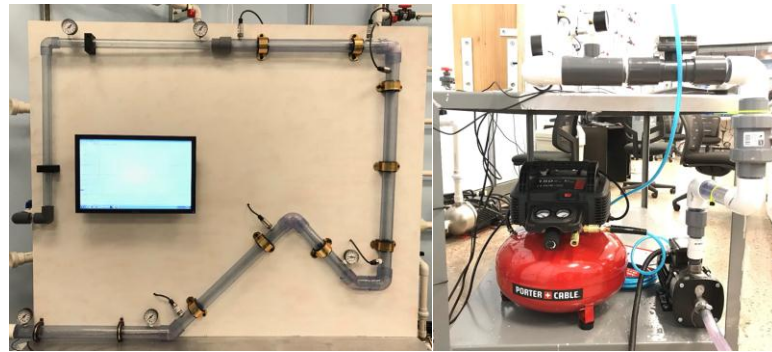


Figure 5: Pipe System Apparatus

(a) (b)

Figure 5: the experimental Setup a) pipe system b) Pipe System continued

The apparatus consists of six pressure transducers each installed before and after each experimental section. Pressure gauges were also installed at the beginning and end of the entire system to monitor the overall pressure losses. As seen in figure 5b a flowmeter was installed before the water/air inlet in order to measure the flowrate of water alone. The same was done with a pressure gauge to measure the air pressure. In order to record data from the pressure transducers, a Data Acquisition was installed to the back of the board. Figure 10 shows the circuit layout used for the installation of the transducers and Data Acquisition.

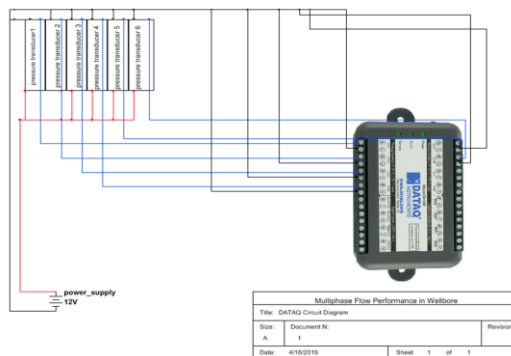


Figure 6: DATAQ and Pressure Transducer Circuit for the project

4. Results

Simulated Velocity Magnitudes

Multiphase velocity magnitudes were simulated for all sections. An inlet mixture velocity of 3.9m/s was used and an outlet pressure of 0psi was used for the outflow. Figures 7-9 show the velocity magnitudes for all the different sections.

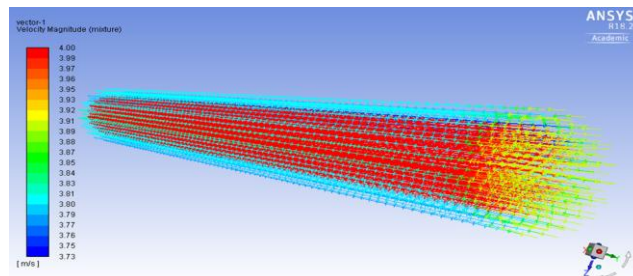


Figure 7: Velocity Magnitude for Horizontal Section

It can be observed that for the horizontal section, a maximum velocity occurs within the pipe at 4.00m/s and decreases throughout the pipe wall linings down to 3.80m/s.

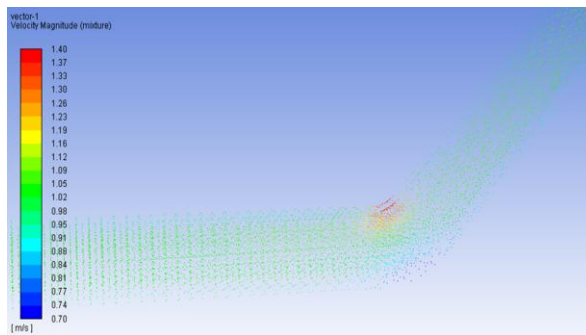


Figure 8: Velocity Magnitude for horizontal to Inclined Section

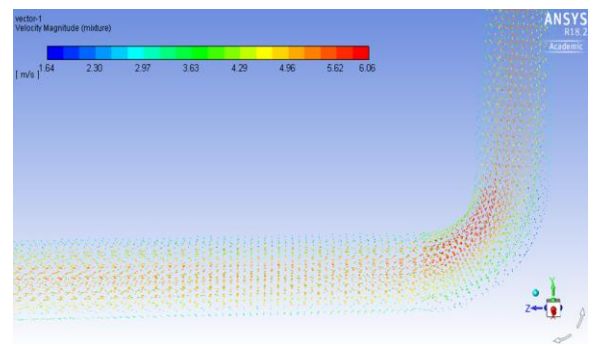


Figure 9: Velocity Magnitude for Horizontal to Vertical Section

For the horizontal to inclined section the velocity magnitude stays constant throughout the pipes and increases to a maximum velocity of 1.40m/s in the pipe fittings. The section changing from horizontal to vertical shows a maximum velocity of 6.06m/s in the pipe fitting and a minimum velocity of 2.30m/s throughout the pipe linings.

Flow Patterns

Experimental results consist of recorded flow patterns for vertical, horizontal and inclined sections. Air pressure was varied in increments of 20psi while the flow was recorded in GPM. Figures 10-12 show the three flow patterns observed throughout the experiments performed. The three flow patterns flow patterns observed were Stratified Wavy, Elongated Bubble and Slug Flow.



Figure 10: Stratified Wavy Flow



Figure 11: Elongated Bubble Flow



Figure 12: Slug Flow

5. Discussion

From our theoretical calculations of pressure loss and pressure drop throughout our system we concluded that the pressure losses are minimal. One main reason for this occurrence is that our system is an open system and our outlet pressure is 0 psi. Similarly, while performing experimental studies of the project we only had minor pressure losses and drops in between the different sections and elbows. We were able to increase the pressure by small fractions by partially closing the choke valve at the outlet of the pipe circuit.

The flow regimes observed were for the most part what we expected to see since previous calculations gave us the conclusion that we can only expect turbulent flow. Therefore, we mostly observed Slug Flow, Elongated Bubble Flow, and Stratified Wavy Flow as seen in Annex B. More specifically, in the horizontal section Stratified Wavy Flow was observed throughout every variation of flow velocity and air pressure. In the vertical section the flow regimes varied between Slug Flow and Elongated Bubble Flow, and for the inclined section the flow regimes also varied

between Slug Flow and Elongated Bubble Flow. Lastly, as seen in Annex C our calculations for pressure losses agree well with the theoretical pressure loss calculations in Annex A.

6. Conclusion

To conclude this paper, we can say that our theoretical results accord with our experimental results. The flow regimes that can be observed agreed well with past multiphase flow experiments. The pressure transducers record minor pressure losses due to an open pipe system. The installed Data Acquisition System can keep track of all minor changes that can be effected by partially closing the choke valve at the outlet. In the future this project can be used as a Laboratory experiment for the Fluid Mechanics Courses.

Nomenclature

e/D = pipe roughness for PVC
 DH = hydraulic pipe diameter
 P_{H_2O} = density of water (liquid)
 μ_{H_2O} = dynamic viscosity of water (liquid)
 m_{H_2O} = mass flowrate of water (liquid)

Acknowledgments

This research study would not have been successful without the help and support of many people around us. First, we would like to thank Mr. Jim McCoy for continuing to support McCoy School of Engineering and all of its research projects.

References

- [1] Journal of Non-Newtonian Fluid Mechanics Volume 127, Issues 2–3, 1 May 2005, Pages 143-155
- [2] Gorgescu, Adelina. AAPP | Physical, Mathematical & Natural Sciences 2017, Vol. 95 Issue 2, p1- 14. 14p. 3 Diagrams, 1 Chart, 1 Graph. DOI: 10.1478/AAPP.952C2.
- [3] Stuhmiller, J.H., 1977. The influence of interfacial pressure forces on the character of the two-phase flow model equations. *Int. J. Multiphase Flow* 3, 551–560.
- [4] Zhang, D.Z., Prosperetti, A., 1997. Momentum and energy equations for disperse two-phase flow and their closure for dilute suspensions. *Int. J. Multiphase Flow* 23, 425–453.
- [5] Pressure Gradient Prediction of Multiphase Flow in Pipes A. Akintola Sarah1, U. Akpabio Julius1,2* and Onuegbu Mary-Ann.
- [6] Predicting Two-Phase Pressure Drops in Vertical Pipe, J. Orkiszewski, Volume 19 Issue 06, 1967.
- [7] Evaluation of Two Phase Flow Characteristics in A Pipeline: Homogenous Model Approach, Okoye Obuora A, *International Journal of Scientific & Technology Research* Vol. 5, Issue 07, July 2016
- [8] S. Farman Ali and H. Yeung. *Experimental Study of Two-Phase Air–Water Flow in Large-Diameter Vertical Pipes*. 2015
- [9] Adapted from J. K. Venard and R. L. Street (1975). *Elementary Fluid Mechanics*, 5th ed., Wiley, New York. At atmospheric pressure.
- [10] Data generated from the EES software developed by S. A. Klein and F. L. Alvarado. Original sources: Keenan, Chao, Keyes, *Gas Tables*, Wiley, 198; and *Thermophysical Properties of Matter*, Vol. 3: Thermal

- Conductivity, Y. S. Touloukian, P. E. Liley, S. C. Saxena, Vol. 11: Viscosity, Y. S. Touloukian, S. C. Saxena, and P. Hestermans, IFI/Plenum, NY, 1970, ISBN 0-306067020-8.
- [11] Pineda-Pérez, H.; Kim, T.; Pereyra, E.; Ratkovich, N. *Chemical Engineering Research & Design: Transactions of the Institution of Chemical Engineers Part A*. Aug2018, Vol. 136, p638-653. 16p. DOI: 10.1016/j.cherd.2018.06.023.
- [12] TWO-phase flow; COMPUTATIONAL fluid dynamics; PARTICLE image velocimetry; LIQUID-vapor interfaces; VISCOSITY; LAMINAR flow
- [13] Li, Mengmeng; Li, Qi; Bi, Gang; Lin, Jiaen. *Mathematical Problems in Engineering*. 9/4/2018, p1-12. 12p. DOI: 10.1155/2018/2896251.
- [14] Ronshin, Fedor. *EPJ Web of Conferences*. 2017, Vol. 159, p1-5. 5p. DOI: 10.1051/epjconf/201715900040.
- [15] Bartkus, German; Kozulin, Igor; Kuznetsov, Vladimir. *EPJ Web of Conferences*. 2017, Vol. 159, p1-4. 4p. DOI: 10.1051/epjconf/201715900004.
- [16] Moutafchieva, Dessislava; Iliiev, Veselin. *Journal of Chemical Technology & Metallurgy*. 2018, Vol. 53 Issue 3, p511-517. 7p.
- [17] Wenwu Zhang; Zhiyi Yu; Baoshan Zhu. *Energies (19961073)*. May2017, Vol. 10 Issue 5, p1-14. 14p. 3 Diagrams, 3 Charts, 9 Graphs. DOI: 10.3390/en10050634.
- [18] Peña-Monferrer, C.; Gómez-Zarzuola, C.; Chiva, S.; Miró, R.; Verdú, G.; Muñoz-Cobo, J. L. *Science & Technology of Nuclear Installations*. 1/16/2018, p1-10. 10p. DOI: 10.1155/2018/2153019.
- [19] Xiao-Ping Chen; Jing-Yu Xu; Jian Zhang. *Chemical Engineering Communications*. 2016, Vol. 203 Issue 9, p1131-1138. 8p. 1 Diagram, 1 Chart, 12 Graphs. DOI: 10.1080/00986445.2016.1160227.
- [20] Fatehi Peikani, A.; Roshani, G.; Fegghi, S. *Instruments & Experimental Techniques*. Sep2017, Vol. 60 Issue 5, p752-758. 7p. DOI: 10.1134/S0020441217050049.
- [21] Vlasák, Pavel; Chára, Zdeněk; Konfršt, Jiří. *EPJ Web of Conferences*. 2018, Vol. 180, p1-6. 6p. DOI: 10.1051/epjconf/201818002120.
- [22] Muszynski, Tomasz; Andrezejczyk, Rafal; Dorao, Carlos A. *Archives of Thermodynamics*. Sep2017, Vol. 38 Issue 3, p101-118. 18p. DOI: 10.1515/aoter-2017-0018.
- [23] Dong, S.; Wang, X. *PLoS ONE*. 5/10/2016, Vol. 11 Issue 5, p1-38. 38p. DOI: 10.1371/journal.pone.0154565.
- [24] Xu, Jingyuan; Lian, Zhanghua; Hu, Jian; Luo, Min. *Energies (19961073)*. Oct2018, Vol. 11 Issue 10, pN.PAG-N.PAG. 1p. DOI: 10.3390/en11102773.
- [25] Farman Ali, S.; Yeung, H. *Chemical Engineering Communications*. Jun2015, Vol. 202 Issue 6, p823-842. 20p. DOI: 10.1080/00986445.2013.879058.
- [26] Kolaas, Jostein; Drazen, David; Jensen, Atle. *Journal of Dispersion Science & Technology*. Oct2015, Vol. 36 Issue 10, p1473-1482. 10p. DOI: 10.1080/01932691.2014.996888.
- [27] Liu, Lei; Jiang, Pingchao; Li, Xiaobai. *Chemical Engineering Communications*. Jul2015, Vol. 202 Issue 7, p864-875. 12p. 2 Diagrams, 1 Chart, 5 Graphs. DOI: 10.1080/00986445.2013.867261.
- [28] Sharar, Darin J.; Bergles, Arthur E.; Jankowski, Nicholas R.; Bar-Cohen, Avram. *Heat Transfer Engineering*. 2016, Vol. 37 Issue 11, p972-984. 13p. 2 Color Photographs, 1 Black and White Photograph, 4 Diagrams, 2 Charts, 3 Graphs. DOI: 10.1080/01457632.2015.1098267.
- [29] Bhagwat, Swanand M.; Ghajar, Afshin J. *Heat Transfer Engineering*. 2015, Vol. 36 Issue 18, p1485-1494. 10p. DOI: 10.1080/01457632.2015.1024979.
- [30] Sharafutdinov, R.; Khabirov, T.; Sadretdinov, A. *Journal of Applied Mechanics & Technical Physics*. Mar2015, Vol. 56 Issue 2, p177-181. 5p. DOI: 10.1134/S0021894415020029.
- [31] Mehta, Hemant B.; Banerjee, Jyotirmay. *Heat Transfer Engineering*. 2015, Vol. 36 Issue 6, p564-573. 10p. 1 Color Photograph, 5 Diagrams, 1 Chart, 4 Graphs. DOI: 10.1080/01457632.2014.939055.
- [32] Huajun Li; Haifeng Ji; Zhiyao Huang; Baoliang Wang; Haiqing Li; Guohua Wu. *Sensors (14248220)*. Feb2016, Vol. 16 Issue 2, p1-13. 13p. DOI: 10.3390/s16020159.
- [33] Haifeng Ji; Huajun Li; Zhiyao Huang; Baoliang Wang; Haiqing Li. *Sensors (14248220)*. 2014, Vol. 14 Issue 12, p22431-22446. 16p. DOI: 10.3390/s141222431.

- [34] Mitrović, Darko; Novak, Andrej. *Mathematical Problems in Engineering*. 3/16/2015, Vol. 2015, p1-8. 8p. DOI: 10.1155/2015/439704.
- [35] Sabzi, Peyman; Noroozi, Saheb. *ASEAN Journal of Chemical Engineering*. 2014, Vol. 14 Issue 1, p13-24. 12p.
- [36] Filip, Alina; Baltaretu, Florin; Damian, Radu-Mircea. *Mathematical Modeling in Civil Engineering*. Dec2014, Issue 4, p22-30. 9p.

Annex

ANNEX A

THEORY SAMPLE CALCULATION

a. Find cross-sectional area, A_c

$$\begin{aligned} A_c &= D_H^2 \\ A_c &= 0.0381^2 \\ A_c &= 0.00145 \text{ m}^2 \end{aligned}$$

b. Find mass flux, j_{H_2O}

$$\begin{aligned} j &= \frac{\dot{m}}{A_c} \\ j &= \frac{0.95}{0.00145} \\ j &= 654.45 \frac{\text{Kg}}{\text{sm}^2} \end{aligned}$$

c. Find Reynolds number, R_{H_2O}

$$\begin{aligned} R_{H_2O} &= \frac{j * D_H}{\mu} \\ R_{H_2O} &= \frac{654.45 * .0381}{0.001002} \\ R_{H_2O} &= 24884.78 \end{aligned}$$

d. Find friction factor, f_{H_2O}

$$\begin{aligned} f_{H_2O}^{-0.5} &= -1.8 \log_{10} \left(\left(\frac{\frac{e}{D}}{3.7 D_H} \right)^{1.11} + \left(\frac{6.9}{R_{H_2O}} \right) \right) \\ f_{H_2O}^{-0.5} &= -1.8 \log_{10} \left(\left(\frac{0.0000015}{3.7 * 0.0381} \right)^{1.11} + \left(\frac{6.9}{24884.78} \right) \right) \\ f_{H_2O}^{-0.5} &= 6.39 \\ f_{H_2O} &= 0.0245 \end{aligned}$$

e. Find pressure gradient, $\left(\frac{\Delta P}{L}\right)_{H_2O}$

$$\begin{aligned} \left(\frac{\Delta P}{L}\right)_{H_2O} &= \frac{f_{H_2O} * (j_{H_2O})^2}{2 * \rho_{H_2O} * D_H} \\ \left(\frac{\Delta P}{L}\right)_{H_2O} &= \frac{0.0245 * (654.45)^2}{2 * 998.2 * 0.0381} \end{aligned}$$

$$\left(\frac{\Delta P}{L}\right)_{H_2O} = 137.96 \text{ Pa/m}$$

Lockhart-Martinelli Calculation

From the Pressure Gradient $\left(\frac{\Delta P}{L}\right)$ the Lockhart-Martinelli parameter, X is given by:

$$X = \sqrt{\frac{\left(\frac{\Delta P}{L}\right)_{H_2O}}{\left(\frac{\Delta P}{L}\right)_{air}}}$$

$$X = \sqrt{\frac{137.96}{0.264}}$$

$$X = 22.86$$

Total Multiphase Pressure Gradient

First the Water Pressure Gradient Multiplier (Chisholm Equation), ϕ_{H_2O} is given by:

$$\phi_{H_2O} = (1 + 18X^{-1} + X^{-2})^{0.5}$$

$$\phi_{H_2O} = (1 + 1822.86^{-1} + 22.86^{-2})^{0.5}$$

$$\phi_{H_2O} = 1.338$$

Then, the Air Pressure Gradient Multiplier (Chisholm Equation) ϕ_{air} , is also given by:

$$\phi_{air} = (1 + 18X^{-1} + X^{-2})^{0.5}$$

$$\phi_{air} = (1 + 1822.86^{-1} + 22.86^{-2})^{0.5}$$

$$\phi_{air} = 1.338$$

Finally the Multiphase Pressure Gradient, $(\Delta P/L)_{multi}$ can be found by the following equation:

$$\left(\frac{\Delta P}{L}\right)_{multi} = \phi_{H_2O}^2 * \left(\frac{\Delta P}{L}\right)_{H_2O} = \phi_{air}^2 * \left(\frac{\Delta P}{L}\right)_{air}$$

$$\left(\frac{\Delta P}{L}\right)_{multi} = 1.338^2 * 137.96 + 1.338^2 * 0.264$$

$$\left(\frac{\Delta P}{L}\right)_{multi} = 247.45 \text{ Pa/m}$$

ANNEX B

EXPERIMENTAL RESULTS

Air Pressure (psi)	Water Flow rate (GPM)	Direction	Pattern
10	0.98	Horizontal	
		Vertical	
		Incline	
	0.65	Horizontal	
		Vertical	
		Incline	
	9.22	Horizontal	
		Vertical	
		Incline	

Air Pressure (psi)	Water Flow rate (GPM)	Direction	Pattern
40	0.98	Horizontal	
		Vertical	
		Incline	
	6.71	Horizontal	
		Vertical	
		Incline	
	9.6	Horizontal	
		Vertical	
		Incline	

Air Pressure (psi)	Water Flow rate (GPM)	Direction	Pattern
20	0.98	Horizontal	
		Vertical	
		Incline	
	6	Horizontal	
		Vertical	
		Incline	
	8.78	Horizontal	
		Vertical	
		Incline	

Air Pressure (psi)	Water Flow rate (GPM)	Direction	Pattern
60	0.98	Horizontal	
		Vertical	
		Incline	
	6.71	Horizontal	
		Vertical	
		Incline	
	9.5	Horizontal	
		Vertical	
		Incline	

Air Pressure (psi)	Water Flow rate (GPM)	Direction	Pattern	Air Pressure (psi)	Water Flow rate (GPM)	Direction	Pattern
80	1.14	Horizontal	 Stratified wavy	120	1.48	Horizontal	 Stratified wavy
		Vertical	 Slug			Vertical	 Slug
		Incline	 Slug			Incline	 Plug
	6.66	Horizontal	 Stratified wavy		6.66	Horizontal	 Stratified wavy
		Vertical	 Slug			Vertical	 Slug
		Incline	 Slug			Incline	 Slug
	9.22	Horizontal	 Stratified wavy		9.33	Horizontal	 Stratified wavy
		Vertical	 Plug			Vertical	 Slug
		Incline	 Plug			Incline	 Slug

Air Pressure (psi)	Water Flow rate (GPM)	Direction	Pattern
100	1.48	Horizontal	 Stratified wavy
		Vertical	 Slug
		Incline	 Slug
	6.66	Horizontal	 Stratified wavy
		Vertical	 Slug
		Incline	 Slug
	9.33	Horizontal	 Stratified wavy
		Vertical	 Slug
		Incline	 Slug

ANNEX C

SAMPLE CALCULATION FOR EXPERIMENTAL PRESSURE LOSS

Water flowrate = 9.33 ft/s

Gas flowrate = 4.82 ft/s was constant

Mass flowrate of water = density × velocity
 = 1.94 × 9.33
 = 18.1 slug/s

Mass flowrate of air = density × velocity
 = 0.0765 × 4.82
 = 0.36 slug/s

Total mass flowrate = mass flowrate of air + mass flowrate water
 = 18.1 + 0.36
 = 18.46 slug/s

b. Find mass flux, j_{H_2O}

$$j = \frac{\dot{m}}{A_c}$$

$$j = \frac{18.1}{0.0038}$$

$$j = 476.3 \frac{\text{slug}}{\text{sft}^2}$$

c. Find Reynolds number, R_{H_2O}

$$R_{H_2O} = \frac{j * D_H}{\mu}$$

$$R_{H_2O} = \frac{476.3 * .0381}{0.001002}$$

$$R_{H_2O} = 18099.78$$

d. Find friction factor,

$$f_{H_2O}^{-0.5} = -1.8 \log_{10} \left(\left(\frac{e}{3.7 D_H} \right)^{1.11} + \left(\frac{6.9}{R_{H_2O}} \right) \right)$$

$$f_{H_2O}^{-0.5} = -1.8 \log_{10} \left(\left(\frac{0.0000015}{3.7 * 0.0381} \right)^{1.11} + \left(\frac{6.9}{24884.78} \right) \right)$$

$$f_{H_2O}^{-0.5} = 4.3$$

$$f_{H_2O} = 0.035$$

e. Find pressure gradient, $\left(\frac{\Delta P}{L} \right)_{H_2O}$

$$\begin{aligned}\left(\frac{\Delta P}{L}\right)_{H_2O} &= \frac{f_{H_2O} * (j_{H_2O})^2}{2 * \rho_{H_2O} * D_H} \\ \left(\frac{\Delta P}{L}\right)_{H_2O} &= \frac{0.035 * (473.6)^2}{2 * 998.2 * 0.0381} \\ \left(\frac{\Delta P}{L}\right)_{H_2O} &= 103.2 \text{ psi/inch}\end{aligned}$$

$$A_c = 0.0381 \text{ in}^2, \quad A_c = 0.00145 \text{ m}^2$$

Find mass flux, j_{air}

$$\begin{aligned}j &= \frac{\dot{m}}{A_c} \\ j &= \frac{0.36}{0.0381} \\ j &= 9.47 \frac{\text{slug}}{\text{s} * \text{ft}^2}\end{aligned}$$

Find Reynolds number, R_{air}

$$\begin{aligned}R_{air} &= \frac{j * D_H}{\mu} \\ R_{air} &= \frac{9.47 * 0.0381}{1.983 * 10^{-5}} \\ R_{air} &= 1819.50\end{aligned}$$

Find friction factor, f_{air}

$$\begin{aligned}f_{air}^{-0.5} &= -1.8 \log_{10} \left(\left(\frac{e}{3.7 D_H} \right)^{1.11} + \left(\frac{6.9}{R_{air}} \right) \right) \\ f_{air}^{-0.5} &= -1.8 \log_{10} \left(\left(\frac{0.0000015}{3.7 * 0.0381} \right)^{1.11} + \left(\frac{6.9}{1819.50} \right) \right) \\ f_{air}^{-0.5} &= 3.17 \\ f_{air} &= 0.0478\end{aligned}$$

Find pressure gradient, $\left(\frac{\Delta P}{L}\right)_{air}$

$$\begin{aligned}\left(\frac{\Delta P}{L}\right)_{air} &= \frac{f_{H_2O} * (j_{air})^2}{2 * \rho_{air} * D_H} \\ \left(\frac{\Delta P}{L}\right)_{air} &= \frac{0.0478 * (9.91)^2}{2 * 1.225 * 0.0381} \\ \left(\frac{\Delta P}{L}\right)_{air} &= 50.2 \text{ psi/ft}\end{aligned}$$